

## **ANALYSIS OF PLANAR MULTILAYER STRUCTURES AT OBLIQUE INCIDENCE USING AN EQUIVALENT BCITL MODEL**

**D. Torrungrueng and S. Lamultree**

Department of Electrical and Electronic Engineering  
Faculty of Engineering and Technology  
Asian University  
Chon Buri, 20150, Thailand

**Abstract**—Planar multilayer structures have found several applications in electromagnetics. In this paper, an equivalent model based on the bi-characteristic-impedance transmission line (BCITL) is employed to model planar multilayer structures effectively for both *lossless* and *lossy* cases. It is found that the equivalent BCITL model provides identical results, for both perpendicular and parallel polarizations, as those obtained from the propagation matrix approach.

### **1. INTRODUCTION**

Multilayer structures have found several applications in electromagnetics; e.g., in the areas of optics, remote sensing and geophysics [1–13], especially for planar multilayer structures. Traditionally, the propagation matrix approach (PMA) is employed to solve problems related to planar multilayer structures rigorously [14]. Alternatively, it is well known that these problems can also be solved readily by modeling these structures using multi-section transmission lines with appropriate characteristic impedances and propagation constants, where each transmission line possesses the same length as of the corresponding layer [15, 16].

Recently, it has been shown that *lossless* multi-section transmission lines can be analyzed successfully using an equivalent model based on the conjugately characteristic-impedance transmission line (CCITL) [17]. By definition, CCITLs are *lossless*, and possess conjugate characteristic impedances of wave propagating in opposite directions. CCITLs can be practically implemented using finite *lossless* periodically loaded transmission lines operated in passbands [18]. However,

CCITLs cannot be used to model *lossy* multi-section transmission lines. Thus, one needs to resort to more general model for these cases.

In this paper, an equivalent model based on the bi-characteristic-impedance transmission line (BCITL) is employed to model planar multilayer structures effectively for both *lossless* and *lossy* cases. In general, BCITLs are *lossy*, and possess different characteristic impedances  $Z_{0b}^{\pm}$  of wave propagating in opposite directions. Note that BCITLs can be practically implemented using finite *lossy* periodically loaded transmission lines, and a graphical tool, known as a *generalized T-chart*, has been recently developed for solving problems associated with BCITLs [19]. It should be pointed out that CCITLs are a special case of BCITLs when associated losses of BCITLs disappear and the passband operation is assumed.

This paper presents the propagation matrix approach in Section 2. Section 3 presents an equivalent model based on BCITLs. Then, numerical results of both approaches are compared in Section 4. Finally, conclusions are provided in Section 5.

## 2. PROPAGATION MATRIX APPROACH

In this section, the propagation matrix approach is discussed for both perpendicular and parallel polarizations. Fig. 1 shows a planar

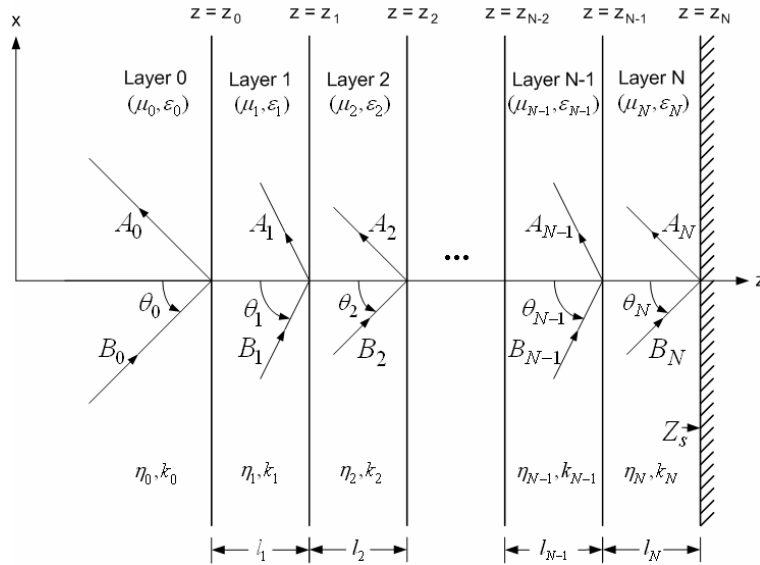


**Figure 1.** Oblique incidence on a planar multilayer structure.

multilayer structure terminated in a surface impedance of  $Z_s$  at  $z = z_N$  and illuminated by a plane wave of oblique incidence of the known amplitude  $B_0$  at the known incident angle  $\theta_0$ . Each layer of length  $l_i$  has the permeability  $\mu_i$ , permittivity  $\varepsilon_i$ , intrinsic impedance  $\eta_i$  and wavenumber  $k_i$ , where  $i = 0, \dots, N$ . At each layer interface,  $B_i$  and  $A_i$  correspond to *unknown* amplitudes ( $B_0$  is known) of incident and reflected waves respectively, and  $\theta_i$  is the *unknown* incident angle ( $\theta_0$  is known), which can be determined from the Snell's law of refraction [14]. These wave amplitudes are associated with electric and magnetic fields for perpendicular and parallel polarizations, respectively. It should be pointed out that  $\mu_0$  and  $\varepsilon_0$  are not necessarily the free space parameters in this notation.

Using the PMA [14], it is found that the wave amplitudes in Layers  $i$  and  $i + 1$  are related by

$$\begin{bmatrix} A_i \\ B_i \end{bmatrix} = [L_i] \begin{bmatrix} A_{i+1} \\ B_{i+1} \end{bmatrix} = \frac{1}{2} \begin{bmatrix} (1+r_i)e^{jk_{z,diff}z_i} & (1-r_i)e^{-jk_{z,sum}z_i} \\ (1-r_i)e^{jk_{z,sum}z_i} & (1+r_i)e^{-jk_{z,diff}z_i} \end{bmatrix} \begin{bmatrix} A_{i+1} \\ B_{i+1} \end{bmatrix}, \quad (1)$$

where

$$k_{z,diff} = k_{z,i+1} - k_{z,i}, \quad (2)$$

$$k_{z,sum} = k_{z,i+1} + k_{z,i}, \quad (3)$$

$$k_{z,i} = k_i \cos \theta_i, \quad (4)$$

$$r_i = \begin{cases} \left( \frac{k_{z,i+1}}{k_{z,i}} \right) \left( \frac{\mu_i}{\mu_{i+1}} \right), & \text{for perpendicular polarization} \\ \left( \frac{k_{z,i+1}}{k_{z,i}} \right) \left( \frac{\varepsilon_i}{\varepsilon_{i+1}} \right), & \text{for parallel polarization.} \end{cases} \quad (5)$$

The total matrix  $[L]$  relating the wave amplitudes in Layers 0 and  $N$  is given in terms of the multiplication of each matrix  $[L_i]$ , where  $i = 0, 1, 2, \dots, N - 1$ , as follows:

$$[L] \triangleq \begin{bmatrix} L_{11} & L_{12} \\ L_{21} & L_{22} \end{bmatrix} = [L_0][L_1][L_2] \dots [L_{N-2}][L_{N-1}]. \quad (6)$$

Once the matrix  $[L]$  is computed by using Eqs. (1) and (6), the total input reflection coefficient  $\Gamma_0$ , defined at the interface between Layers 0 and 1, can be determined in terms of each element of  $[L]$  as

$$\Gamma_0 \triangleq \frac{A_0}{B_0} = \frac{L_{11}R_N e^{-j2k_{z,N}z_N} + L_{12}}{L_{21}R_N e^{-j2k_{z,N}z_N} + L_{22}}, \quad (7)$$

where

$$R_N = \begin{cases} \frac{k_{z,N}Z_s - \omega\mu_N}{k_{z,N}Z_s + \omega\mu_N}, & \text{for perpendicular polarization} \\ \frac{k_{z,N}Y_s - \omega\varepsilon_N}{k_{z,N}Y_s + \omega\varepsilon_N}, & \text{for parallel polarization} \end{cases}, \quad (8)$$

and  $Y_s = Z_s^{-1}$  is the surface admittance at  $z = z_N$ . In the next section, the equivalent model based on BCITLs is developed for planar multilayer structures.

### 3. EQUIVALENT MODEL BASED ON BCITLS

As pointed out earlier, planar multilayer structures can be analyzed by modeling these structures using multi-section transmission lines. Fig. 2(a) illustrates the equivalent multi-section model of Fig. 1, where the propagation constant  $\beta_i$  and the characteristic impedance  $Z_i$  of each transmission line in the multi-section model are defined as

$$\beta_i = k_{z,i}, \quad (9)$$

$$Z_i = \begin{cases} \eta_i \sec \theta_i, & \text{for perpendicular polarization} \\ \eta_i \cos \theta_i, & \text{for parallel polarization} \end{cases}. \quad (10)$$

The multi-section model can be analyzed effectively using the BCITL model shown in Fig. 2(b). In [17] and [20], the characteristic impedances  $Z_{0b}^{\pm}$  and the propagation constant  $\beta_b$  can be determined from the total transmission ( $ABCD$ ) matrix of the *cascading*  $N$ -section transmission lines of the total length  $l_T$  in Fig. 2(a) as

$$Z_{0b}^{\pm} = \frac{\mp 2B}{(A - D) \mp j\sqrt{4 - (A + D)^2}} \quad (11)$$

$$\cos(\beta_b l_T) = \frac{A + D}{2}. \quad (12)$$

Note that the formula of the  $ABCD$  matrix of each  $N$ -section transmission line is provided in [20].

Using the theory of two-port network [20], it can be shown rigorously that the two transmission line models in Fig. 2 are equivalent; i.e., their total transmission matrices are identical. It should be pointed out that the BCITL model is equivalent to the multi-section model at the input and output terminals only; i.e., at

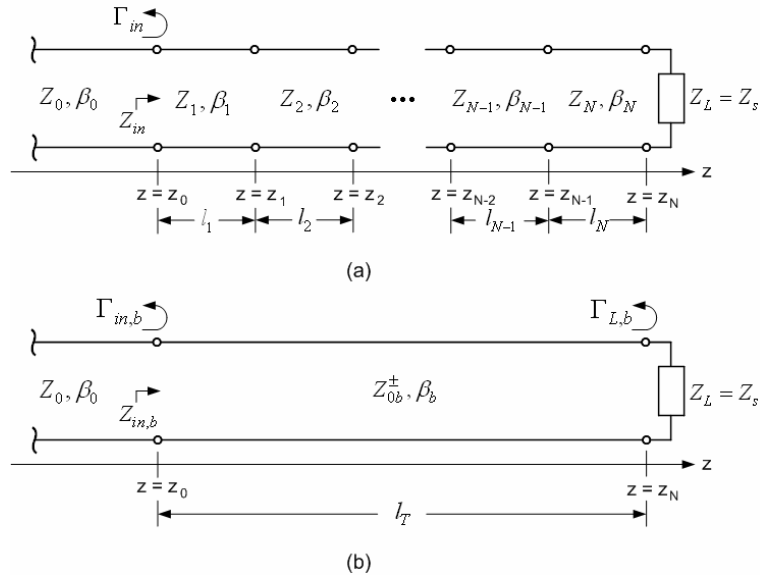


**Figure 2.** Transmission line models: (a) Multi-section model and (b) BCITL model.

$z = z_0$  and  $z = z_N$  respectively as shown in Fig. 2. This is due to the fact that the multi-section transmission line in Fig. 2(a) is globally viewed as a two-port network in constructing the BCITL model.

The total input reflection coefficient  $\Gamma_{in,b}$  in Fig. 2(b) can be determined from the input impedance  $Z_{in,b}$  as

$$\Gamma_{in,b} = \pm \left[ \frac{Z_{in,b} - Z_0}{Z_{in,b} + Z_0} \right], \quad (13)$$

where

$$Z_{in,b} = Z_{0b}^+ Z_{0b}^- \left[ \frac{1 + \Gamma_{L,b} e^{-j2\beta_b l_T}}{Z_{0b}^- - Z_{0b}^+ \Gamma_{L,b} e^{-j2\beta_b l_T}} \right] \quad (14)$$

$$\Gamma_{L,b} = \frac{Z_s Z_{0b}^- - Z_{0b}^+ Z_{0b}^-}{Z_s Z_{0b}^+ + Z_{0b}^+ Z_{0b}^-}. \quad (15)$$

The derivation of  $Z_{in,b}$  and  $\Gamma_{L,b}$  can be found in [21]. Note that the load reflection coefficient  $\Gamma_{L,b}$  associated with the BCITL is defined at  $z = z_N$ . In Eq. (13), the *plus* and *minus* signs correspond to the perpendicular and parallel polarizations, respectively. The *minus* sign comes from the fact that the total input reflection coefficient is

associated with the *current*, instead of the voltage, for the parallel polarization. In the next section, numerical results of both approaches are compared.

#### 4. NUMERICAL RESULTS

For illustration of the validity of the equivalent BCITL model, consider a *lossy* planar three-layer structure ( $N = 3$ ) illuminated by an oblique plane wave at 18 GHz and terminated in a surface impedance of  $Z_s = 50.0\Omega$ . Parameters of each layer are given as follows:  $\mu_{r,0} = \mu_{r,1} = \mu_{r,2} = \mu_{r,3} = 1.0$ ,  $\varepsilon_{r,0} = 1.0$ ,  $\varepsilon_{r,1} = 5.0 - j0.01$ ,  $\varepsilon_{r,2} = 10.0 - j0.05$ ,  $\varepsilon_{r,3} = 14.0 - j0.01$ ,  $z_0 = 0.0$  m,  $z_1 = 0.10$  m,  $z_2 = 0.15$  m and  $z_3 = 0.30$  m.

For the perpendicular polarization, Figs. 3 and 4 illustrate the plots of the magnitude and phase of the characteristic impedances  $Z_{0b}^{\pm}$  computed by using Eq. (11) versus the incident angle  $\theta_0$ , respectively. Note that  $Z_{0b}^+$  and  $Z_{0b}^-$  are generally complex and different. These results are consistent with the fact that the structure of interest is *lossy*. In addition,  $Z_{0b}^{\pm}$  vary considerably with  $\theta_0$ . Fig. 5 shows the plot of the real and imaginary parts of the propagation constant  $\beta_b$  versus  $\theta_0$ . Note that  $\beta_b$  is also complex in general due to the *lossy* structure of interest, and it varies noticeably with  $\theta_0$ . Fig. 6 shows the plot of the magnitude of the total input reflection coefficient versus  $\theta_0$  for both PMA ( $\Gamma_0$ ) and equivalent BCITL model ( $\Gamma_{in,b}$ ). It is obvious that numerical results obtained from both approaches are identical for

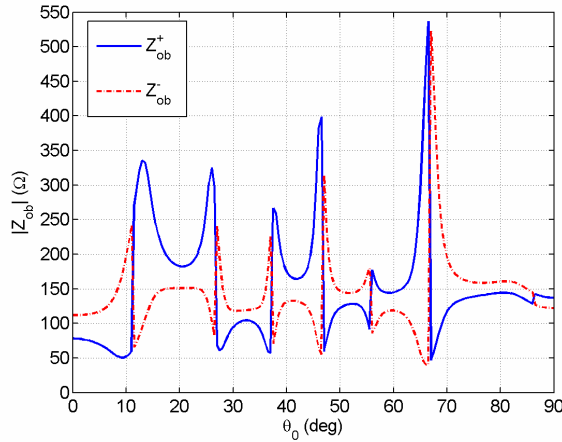


**Figure 3.** Plot of the magnitude of the characteristic impedances  $Z_{0b}^{\pm}$  versus  $\theta_0$  for the perpendicular polarization.

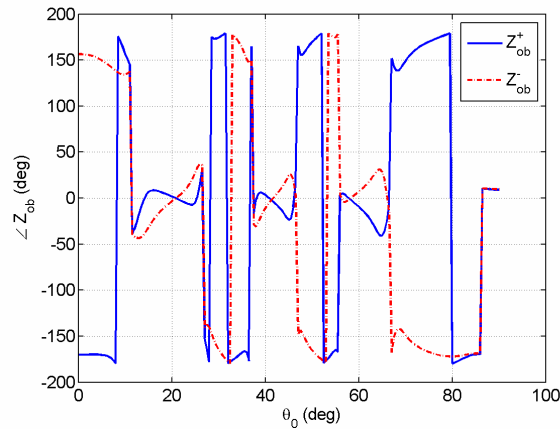


**Figure 4.** Plot of the phase of the characteristic impedances  $Z_{0b}^{\pm}$  versus  $\theta_0$  for the perpendicular polarization.

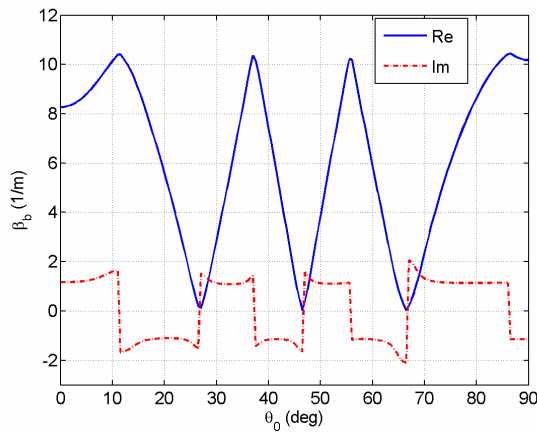


**Figure 5.** Plot of the real and imaginary parts of the propagation constant  $\beta_b$  versus  $\theta_0$  for the perpendicular polarization.

all  $\theta_0$  of interest.

For the parallel polarization, Figs. 7 and 8 show the plots of the magnitude and phase of the characteristic impedances  $Z_{0b}^{\pm}$  versus the incident angle  $\theta_0$ , respectively. As in the case of the perpendicular polarization,  $Z_{0b}^+$  and  $Z_{0b}^-$  are generally complex and different, and they vary considerably with  $\theta_0$ . Note that  $Z_{0b}^{\pm}$  for perpendicular and parallel polarizations are generally different as expected. Fig. 9 illustrates the

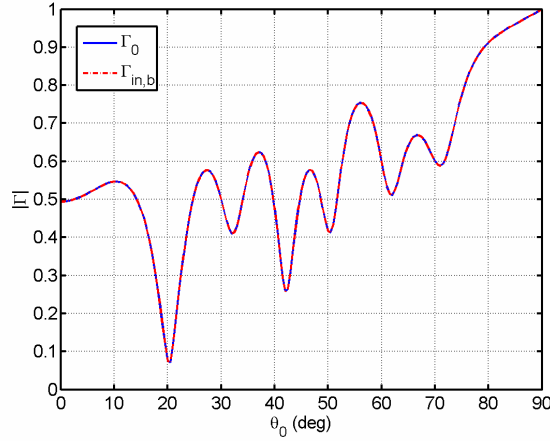


**Figure 6.** Plot of the magnitude of the total input reflection coefficient versus  $\theta_0$  for the perpendicular polarization.

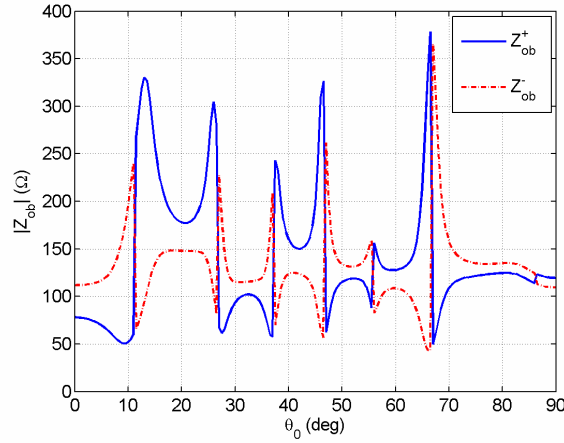


**Figure 7.** Plot of the magnitude of the characteristic impedances  $Z_{0b}^{\pm}$  versus  $\theta_0$  for the parallel polarization.

plot of the real and imaginary parts of the propagation constant  $\beta_b$  versus  $\theta_0$ . As in the case of the perpendicular polarization,  $\beta_b$  is also complex, and it varies noticeably with  $\theta_0$ . It should be pointed out that  $\beta_b$  in Figs. 5 and 9 are different although they look very similar. Fig. 10 shows the plot of the magnitude of the total input reflection coefficient versus  $\theta_0$  for both PMA ( $\Gamma_0$ ) and equivalent BCITL model ( $\Gamma_{in,b}$ ). Note that numerical results obtained from both approaches are identical for all  $\theta_0$  of interest.

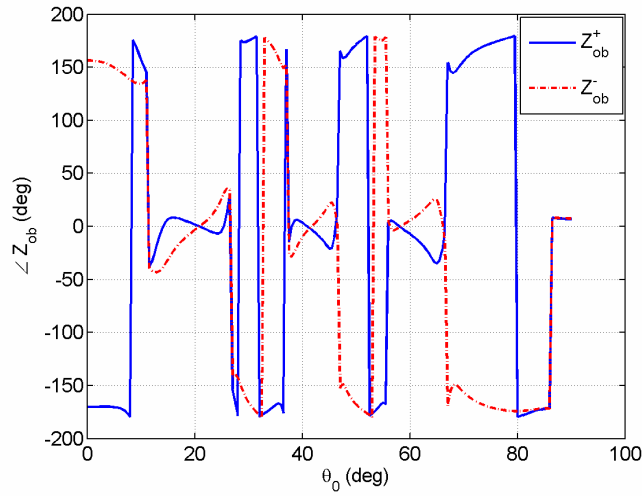


**Figure 8.** Plot of the phase of the characteristic impedances  $Z_{0b}^{\pm}$  versus  $\theta_0$  for the parallel polarization.

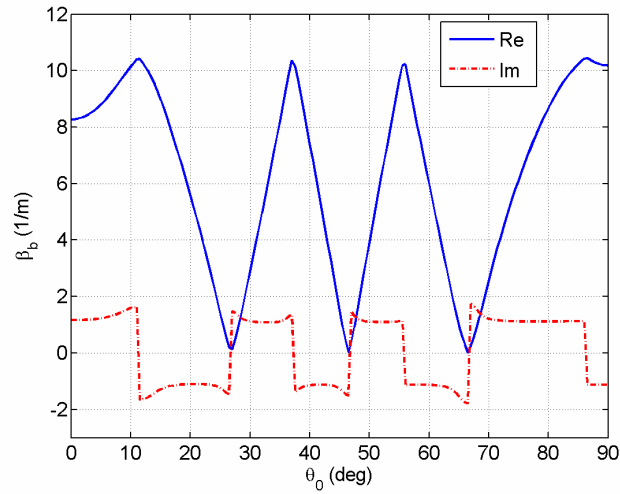


**Figure 9.** Plot of the real and imaginary parts of the propagation constant  $\beta_b$  versus  $\theta_0$  for the parallel polarization.

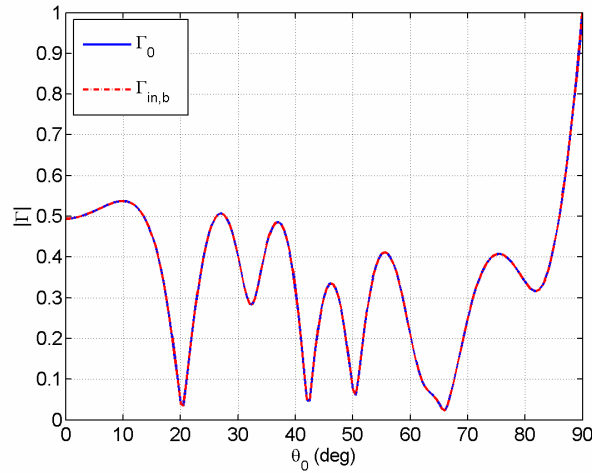


**Figure 10.** Plot of the magnitude of the total input reflection coefficient versus  $\theta_0$  for the parallel polarization.

## 5. CONCLUSIONS

Planar multilayer structures at oblique incidence can be analyzed successfully using an equivalent BCITL model for both perpendicular and parallel polarizations. The variations of BCITL parameters,  $Z_{0b}^{\pm}$  and  $\beta_b$ , with the incident angle  $\theta_0$  are studied as well. It is found that these parameters are generally complex and strongly dependent on  $\theta_0$  for both polarizations. In addition, the magnitude of the total input reflection coefficient obtained from both PMA and equivalent BCITL model are identical indeed. Finally, the equivalent BCITL model is conceptually simple and effective, and may offer better physical insight into more complicated multilayer structures.

## REFERENCES

1. Qing, A. and C. K. Lee, "An improved model for full wave analysis of multilayered frequency selective surface with gridded square element," *Progress In Electromagnetics Research*, PIER 30, 285–303, 2001.
2. Kong, J. A., "Electromagnetic wave interaction with stratified negative isotropic media," *Progress In Electromagnetics Research*, PIER 35, 1–52, 2002.
3. Khalaj-Amirhosseini, M., "Analysis of lossy inhomogeneous

- planar layers using Taylor's series expansion," *IEEE Trans. Antennas and Propagation*, Vol. 54, No. 1, 130–135, Jan. 2006.
4. Khalaj-Amirhosseini, M., "Analysis of lossy inhomogeneous planar layers using finite difference method," *Progress In Electromagnetics Research*, PIER 59, 187–198, 2006.
  5. Rothwell, E. J., "Natural-mode representation for the field reflected by an inhomogeneous conductor-backed material layer – TE case," *Progress In Electromagnetics Research*, PIER 63, 1–20, 2006.
  6. Kedar, A. and U. K. Revankar, "Parametric study of flat sandwich multilayer Radome," *Progress In Electromagnetics Research*, PIER 66, 253–265, 2006.
  7. Aissaoui, M., J. Zaghdoudi, M. Kanzari, and B. Rezig, "Optical properties of the quasi-periodic one-dimensional generalized multilayer fibonacci structures," *Progress In Electromagnetics Research*, PIER 59, 69–83, 2006.
  8. Khalaj-Amirhosseini, M., "Analysis of lossy inhomogeneous planar layers using equivalent sources method," *Progress In Electromagnetics Research*, PIER 72, 61–73, 2007.
  9. Khalaj-Amirhosseini, M., "Analysis of lossy inhomogeneous planar layers using the method of moments," *Journal of Electromagnetic Waves and Applications*, Vol. 21, No. 14, 1925–1937, 2007.
  10. Khalaj-Amirhosseini, M., "Analysis of lossy inhomogeneous planar layers using fourier series expansion," *IEEE Trans. Antennas and Propagation*, Vol. 55, No. 2, 489–493, Feb. 2007.
  11. Suyama, T., Y. Okuno, A. Matsushima, and M. Ohtsu, "A numerical analysis of stop band characteristics by multilayered dielectric gratings with sinusoidal profile," *Progress In Electromagnetics Research B*, Vol. 2, 83–102, 2008.
  12. Yildiz, C. and M. Turkmen, "Quasi-static models based on artificial neural networks for calculating the characteristic parameters of multilayer cylindrical coplanar waveguide and strip line," *Progress In Electromagnetics Research B*, Vol. 3, 1–22, 2008.
  13. Oraizi, H. and A. Abdolali, "Combination of MLS, GA & CG for the reduction of RCS of multilayered cylindrical structures composed of dispersive metamaterials," *Progress In Electromagnetics Research B*, Vol. 3, 227–253, 2008.
  14. Kong, J. A., *Electromagnetic Wave Theory*, 2nd edition, Wiley-Interscience, NY, 1990.
  15. Wait, J. R., *Electromagnetic Wave Theory*, John Wiley & Son,

- Sigapore, 1989.
16. Oraizi, H. and M. Afsahi, "Analysis of planer dielectric multilayers as FSS by transmission line transfer matrix method (TLTMM)," *Progress In Electromagnetics Research*, PIER 74, 217–240, 2007.
  17. Worasawate, D. and D. Torrungrueng, "Analysis of a multi-section impedance transformer using an equivalent CCITL model," *Proc. of the 2006 ECTI-CON*, 111–114, Ubon Ratchatani, Thailand, May 10–13, 2006.
  18. Torrungrueng, D., C. Thimaporn, and N. Chamnandechakun, "An application of the T-chart for solving problems associated with terminated finite lossless periodic structures," *Microwave and Optical Tech. Lett.*, Vol. 47, No. 6, 594–597, December 2005.
  19. Torrungrueng, D., P. Y. Chou, and M. Krairiksh, "A graphical tool for analysis and design of bi-characteristic-impedance transmission lines," *Microwave and Optical Tech. Lett.*, Vol. 49, No. 10, 2368–2372, October 2007.
  20. Pozar, D. M., *Microwave Engineering*, 3rd edition, Wiley, NJ, 2005.
  21. Torrungrueng, D. and C. Thimaporn, "A generalized ZY Smith chart for solving nonreciprocal uniform transmission-line problems," *Microwave and Optical Tech. Lett.*, Vol. 40, No. 1, 57–61, January 2004.